DEUTSCHES ELEKTRONEN-SYNCHROTRON DESY

DESY 85-112
October 1985

SNEUTRINO COUNTING

by

J.A. Grifols

Dept. de Física Teórica, Univ. Autónoma de Barcelona, Bellaterra

M. Martinez, J. Solà

Deutsches Elektronen-Synchrotron DESY, Hamburg

ISSN 0418-9833

NOTKESTRASSE 85 · 2 HAMBURG 52

To be sure that your preprints are promptly included in the
HIGH ENERGY PHYSICS INDEX ,
send them to the following address (if possible by air mail) :

DESY
Bibliothek
Notkestrasse 85
2 Hamburg 52
Germany

DESY 85-112
October 1985

ISSN 0418-9833

SNEUTRINO COUNTING[o]

J.A. Grifols
Departament de Física Teórica
Universitat Autònoma de Barcelona
Bellaterra (Barcelona) Spain

M. Martínez[+] and J. Solà[++]
Deutsches Elektronen-Synchrotron
DESY, Hamburg

ABSTRACT: We give a detailed analysis of the reaction $e^+e^- \to \gamma\bar{\nu}\nu$. If the sneutrino is the lightest supersymmetric particle, detecting a single photon plus missing energy provides an excellent tool for either discover new physics or for setting interesting bounds on the masses of the sneutrino and the wino.

[o] Work partially supported by research projects CAICYT

[+] Junta de Energia Nuclear. On leave of absence from the "Laboratori de Física d'Altes Energies", Bellaterra (Barcelona), Spain.

[++] On leave from the Facultat de Veterinária de la Universitat Autónoma de Barcelona.

1. INTRODUCTION

Establishing Supersymmetry (SUSY) experimentally is obviously an endeavour of paramount importance. Equally important, however, is to establish the absence of SUSY at every stage of experimentally accessible energies. Indeed, it is very useful for model building that the exclusion - or eventual discovery, of course - of supersymmetric signals is carried out thoroughly and systematically: in such a way that one can be reasonable certain of not having missed a positive signal and thus, such that (lower) bounds on SUSY masses and mixing parameters can be reliably set. Up to now no conclusive evidence for SUSY has emerged from accelerator data either in e^+e^- interactions nor in $p\bar{p}$ interactions, but already useful limits on supersymmetric particle masses have been given from the analysis of the different existing experiments. A powerful method that has been used in e^+e^- collisions - e. g. to set the best limits on the selectron mass[1] - is to look for single photons in the final state with no other particle being detected[2-4]. In the process stable neutral particles must be produced. They might be neutrinos. In fact, this is a well known technique for counting neutrino species. But they might be more exotic particles like photinos or sneutrinos. Various SUSY models predict the sneutrino to be the lightest SUSY particle (LSP) and being thus stable[5-7]. In this case the method just mentioned should provide useful information concerning supersymmetry. In fact, the method should be able to discriminate between the standard 3 family contribution and any additional contribution due to supersymmetric particles. It was actually used - PEP data were used - to set limits on sneutino masses within a class of supergravity models[8].

In the present paper we reexamine the process $e^+e^- \to \gamma\bar{\nu}\nu$ more thoroughly. For two reasons: firstly, because the existing literature on the subject differs nummerically by (roughly) a factor of two in the region of PEP and PETRA energies[2,8]. This should be clarified for obvious reasons. The second reason is that we wish to give a more complete survey of the process as required by the analysis of recent and future experiments.

In particular we want to use the recent single photon data[9] from the ASP collaboration at the PEP machine which were presented by M. J. Jonker at the DESY Workshop last October.

In the next section (section 2) we give the necessary framework and the amplitudes for the process $e^+e^- \to \gamma\tilde{\nu}\bar{\tilde{\nu}}$. We conclude with section 3, which is devoted to the discussion of the numerical results.

2. FRAMEWORK AND AMPLITUDES

In general, mass eigenstates of SUSY particles are not weak eigenstates. The scalar partners of left handed and right handed quarks (and leptons) are mixed among each other. So are the partners of gauge bosons and Higgs bosons. Indeed, the mass eigenstates for SUSY fermions are mixtures of higgsinos - the partners of Higgs bosons - and winos and zinos - the partners of gauge bosons - with mixing angles which depend on the relative strength of the different supersymmetry and SU(2)xU(1) breaking parameters[10].

In a model with no right handed neutrinos, however, the partner of the left handed neutrino, the sneutrino $\tilde{\nu}_L$, is a mass eigenstate. Furthermore, in models where the sneutrino is the LSP, one ends up with a light chargino state (charged gauge SUSY fermion) which is almost a weak eigenstate - a wino - and a charged heavy chargino (an almost pure higgsino state). This last one decouples for any practical purpose from electron interactions[7,8,10]. Only the light wino will play a role in our process.

The amplitudes that participate in the process $e^+e^- \to \gamma\tilde{\nu}\bar{\tilde{\nu}}$ are displayed in fig. 1. The first three amplitudes involve apart from the electromagnetic vertex, the interaction[7].

$$\mathcal{L} = ig\cos\phi\,\bar{e}_L\tilde{W}^c\tilde{\nu}_L + \text{h.c.} \qquad (1)$$

where $\tilde{W}$ is the (light) wino field and ϕ is the mixing angle, which we shall take from now on such that $\cos\phi = 1$.

The last two amplitudes in fig. 1 involve the $Z\tilde{\nu}\bar{\tilde{\nu}}$ vertex[7].

$$\mathcal{L}' = \frac{ig}{2\cos\theta_W}\,\tilde{\nu}_L^+ \overleftrightarrow{\partial_\mu}\,\tilde{\nu}_L\, Z^\mu \qquad (2)$$

and the familiar standard model couplings to electrons.

It is now straightforward to write down the explicit formulae for the five amplitudes. They read,

$$T_1 = ieg^2\left[\bar{e}^+(p_1)\not{\epsilon}(\not{p}_3-\not{p}_1)\cdot\not{p}_4 P_L e^-(p_2)\right]\left[(p_3-p_1)^2-m_e^2\right]^{-1}$$
$$\left[(p_2-p_4)^2-M_{\tilde{W}}^2\right]^{-1} \qquad (3a)$$

$$T_2 = -ieg^2\left[\bar{e}^+(p_1)\not{p}_3(\not{p}_2-\not{p}_3)\not{\epsilon}P_L e^-(p_2)\right]\left[(p_3-p_1)^2-M_{\tilde{W}}^2\right]^{-1}$$
$$\left[(p_2-p_3)^2-m_e^2\right]^{-1} \qquad (3b)$$

$$T_3 = -ieg^2\left[\bar{e}^+(p_1)P_R(\not{p}_3+M_{\tilde{W}})\not{\epsilon}(-\not{p}_4+M_{\tilde{W}})P_L e^-(p_2)\right]\left[(p_3-p_1)^2-\right.$$
$$\left.-M_{\tilde{W}}^2\right]^{-1}\left[(p_2-p_4)^2-M_{\tilde{W}}^2\right]^{-1} \qquad (3c)$$

$$T_4 = \frac{ieg^2}{2\cos^2\theta_W}\left[\bar{e}^+(p_1)\not{\epsilon}(\not{p}_3-\not{p}_1)(\not{p}_4-\not{p}_3)(C_e^L P_L + C_e^R P_R)e^-(p_2)\right]$$
$$\left[(p_3-p_1)^2-m_e^2\right]^{-1}\left[(p_4+p_3)^2-M_Z^2+i\varepsilon\right]^{-1} \qquad (3d)$$

$$T_5 = \frac{ieg^2}{2\cos^2\theta_W}\left[\bar{e}^+(p_1)(\not{p}_4-\not{p}_3)(C_e^L P_L + C_e^R P_R)(\not{p}_2-\not{p}_3)\not{\epsilon}e^-(p_2)\right]$$
$$\left[(p_2-p_3)^2-m_e^2\right]^{-1}\left[(p_4+p_3)^2-M_Z^2+i\varepsilon\right]^{-1} \qquad (3e)$$

where $P_{R,L} = \frac{1}{2}(1\pm\gamma_5)$, $C_e^L = \sin^2\theta_W - \frac{1}{2}$, $C_e^R = \sin^2\theta_W$, ϵ^μ is the polarization vector of the photon and $\varepsilon \equiv M_Z\,\Gamma_Z$.

Having stated the amplitudes we can now turn to the cross sections.

3. RESULTS

We have used the REDUCE programme to square the amplitudes and the adaptative multidimensional integration algorithm VEGAS [11] to perform phase space integrals. To comply with experimental requirements we applied the the following cuts. The photon angle θ_γ to the beam axis is constrained to lie between $20^0 < \theta_\gamma < 160^0$ and its transverse momentum p_T is bound to be larger than $.1\sqrt{s}$.

These cuts are useful, not only for experimental purposes, but also because they are performed on suitable laboratory variables which are constrained to vary in a region where unnecessary peaking effects are avoided. And in fact, we have rechecked our phase space integrals using an ordinary gaussian routine and we obtained the same results.

Fig. 2 shows the total cross section for $e^+e^- \to \gamma\nu\bar{\nu}$ (summed over 3 families) as a function of the C.M. energy $\sqrt{s}$. Also shown on fig. 2 are the cross sections for photino production $\tilde{e}\tilde{e} \to \gamma\tilde{\gamma}\tilde{\gamma}$ and for the standard model process $e\bar{e} \to \gamma\nu\bar{\nu}$ (3 generations). The selectron mass is taken to be 30 GeV and the wino mass 25 GeV. Both values correspond roughly to the minimum masses allowed by experiment. We see that the process under scrutiny has the largest cross section over a range of energies that extend up to approximately the Z^0-boson mass. The process involving photinos is almost flat over the entire range of energies since there is no Z^0 exchange contributing. The other two processes - neutrino and sneutrino production - show the typical rise associated to s-channel Z^0 exchange. If we compare the curve for $\sigma(e^+e^- \to \gamma\tilde{\nu}\bar{\tilde{\nu}})$ with the corresponding curve in ref. (8) we see that, as already mentioned in the introduction, our results are more than a factor of two smaller in the PEP and PETRA energy domain (around 30 and 40 GeV, respectively).

The curves shown in fig. 2 have been obtained considering the photino and the sneutrino to be massless. We may now see the effect of a nonzero mass for the sneutrino. Figs. 3, 4 and 5 show the cross section $\sigma(e^+e^- \to \gamma\tilde{\nu}\bar{\tilde{\nu}})$ as a function of sneutrino mass for $\sqrt{s}$ = 44 GeV (PETRA), $\sqrt{s}$ = 93 GeV (at the Z^0 pole; LEP) and $\sqrt{s}$ = 160 GeV (LEP II), respectively. The wino mass has been taken to be 25, 40 and 90 GeV, respectively, i. e. always larger than the corresponding range of masses permitted to the sneutrino (LSP).

We may fix the mass of the sneutrino to be zero and vary the mass of the wino. This we display in figs. 6, 7 and 8 where the cross section for $e^+e^- \to \gamma\nu\bar{\nu}$ is given at the three energies 44 GeV, 93 GeV and 160 GeV as a function of $M_{\tilde{W}}$.

To assess the detection possibilities of this process and to help put limits on SUSY masses we plot on the $M_{\tilde{W}}$-$M_{\tilde{\nu}}$ plane two pairs of curves (see fig. 9). Curves (a) and (b) have been obtained by just applying the same kinematic cuts than those performed on the aforementioned recent data from the ASP collaboration [9], i. e., the photon angle is constrained to lie between $20 < \theta_\gamma < 160$ as before, but its transverse momentum is required to be larger than 1 GeV ($\sqrt{s}$ = 29 GeV at PEP). The inner region delimitated by curve (a) and the axes corresponds to rates of $\gamma\nu\bar{\nu}$ production that exceed 1 event for an integrated luminosity of 100 pb^{-1}, i. e., all pairs of masses $(M_{\tilde{W}}, M_{\tilde{\nu}})$ inside the area bound by this curve should be excluded at the 1 evt/100 pb^{-1} level. Similarly the inner domain defined by curve (b) corresponds to rates of $\gamma\nu\bar{\nu}$ production that exceed 3 events for the very same integrated luminosity. With this second curve we account for the $(M_{\tilde{W}}, M_{\tilde{\nu}})$ bounds at the 95 % C.L. of the Poisson distribution, i.e., no reasonable possibility is left in this case to statistical fluctuations. Finally, curves (c) and (d) have a similar interpretation as the two previous ones but they correspond to the range that could be (optimistically) covered by PETRA. The cut on the photon angle is again the same as before but its transverse momentum is bound to be larger than 4.4 GeV (= $0.1\sqrt{s}$).

The analysis by the authors of ref. [9] was carried out over an integrated luminosity of 68.7 pb^{-1}, which was collected all along this year. It then follows from our calculations that if no clear single photon candidate is observed by ASP when it soon will be reaching 100 pb^{-1}, then we shall be able to exclude a good bit of the $M_{\tilde{W}}$-$M_{\tilde{\nu}}$ plane (fig. 9). In particular, if $m_{\tilde{\nu}} = 0$ then we would infer from curve (b) that $M_{\tilde{W}} \geq 65$ GeV at the 95 % C.L.

We conclude with a few words on background. The signature for the process is quite clear, a single photon plus missing energy. Events with additional charged particles must be vetoed. However, a 4π coverage of the interaction volume is impossible in practice. Therefore, in addition to the genuine photon + invisible energy background processes, like

$e\bar{e} \to \gamma\nu\bar{\nu}$ or $e\bar{e} \to \gamma\tilde{\gamma}\bar{\tilde{\gamma}}$ one has to cope with other competing processes, like Beam-Beam Bremsstrahlung (BBB) or $e\bar{e} \to 3\gamma$ where the extra particles are missed by the detectors (e. g., they may escape along the beam pipe). The question of background to the standard process ($e\bar{e} \to \gamma\nu\bar{\nu}$) has been studied carefully in the literature[12]. The most serious one is Beam-Beam bremsstrahlung. It should not be a problem in our case for, in the PETRA energy range, the cross section for $e^+e^- \to \gamma\tilde{\nu}\bar{\tilde{\nu}}$ is almost two orders of magnitude larger than the one for $e^+e^- \to \gamma\nu\bar{\nu}$ and, in the high energy region (above the Z^0 pole) it was already shown in our previous analysis that BBB could be kept under control (the present numerical results agree with those in ref. (2)). In any case the absence of signal at the expected rate will provide unquestionable - independent of background - bounds on SUSY parameters.

ACKNOWLEDGEMENTS

Two of us (M.M. and J.S.) would like to acknowledge, respectively, the Spanish Junta de Energía Nuclear and the Ministerio de Educación y Ciencia for financial support.

We would also thank professor R.D. Peccei for drawing our attention upon the new ASP data and for various useful suggestions to our original manuscript.

FIGURE CAPTIONS

FIG.1.- Diagrams contributing to $e^+e^- \to \gamma\tilde{\nu}\bar{\tilde{\nu}}$.

FIG.2.- Cross sections for i) $e^+e^- \to \gamma\tilde{\nu}\bar{\tilde{\nu}}$ (full line), ii) $e^+e^- \to \gamma\tilde{\gamma}\bar{\tilde{\gamma}}$ (dash-dotted line) and iii) $e^+e^- \to \gamma\nu\bar{\nu}$ (dashed line) as a function of $\sqrt{s}$. $M_{\tilde{e}}$=30 GeV, $M_{\tilde{W}}$=25 GeV, $M_{\tilde{\gamma}}=M_{\tilde{\nu}}=0$.

FIG.3.- $\sigma(e\bar{e} \to \gamma\tilde{\nu}\bar{\tilde{\nu}})$ for $\sqrt{s}$=44 GeV as a function of $M_{\tilde{\nu}}$. $M_{\tilde{W}}$=25 GeV.

FIG.4.- $\sigma(e\bar{e} \to \gamma\tilde{\nu}\bar{\tilde{\nu}})$ for $\sqrt{s}$=93 GeV as a function of $M_{\tilde{\nu}}$. $M_{\tilde{W}}$=40 GeV.

FIG.5.- $\sigma(e\bar{e} \to \gamma\tilde{\nu}\bar{\tilde{\nu}})$ for $\sqrt{s}$=160 GeV as a function of $M_{\tilde{\nu}}$. $M_{\tilde{W}}$=90 GeV.

FIG.6.- $\sigma(e\bar{e} \to \gamma\tilde{\nu}\bar{\tilde{\nu}})$ for $\sqrt{s}$=44 GeV as a function of $M_{\tilde{W}}$. $M_{\tilde{\nu}}$=0.

FIG.7.- $\sigma(e\bar{e} \to \gamma\tilde{\nu}\bar{\tilde{\nu}})$ for $\sqrt{s}$=93 GeV as a function of $M_{\tilde{W}}$. $M_{\tilde{\nu}}$=0.

FIG.8.- $\sigma(e\bar{e} \to \gamma\tilde{\nu}\bar{\tilde{\nu}})$ for $\sqrt{s}$=160 GeV as a function of $M_{\tilde{W}}$. $M_{\tilde{\nu}}$=0.

FIG.9.- The $M_{\tilde{W}}$ - $M_{\tilde{\nu}}$ plane. All pairs inside the areas bound by the curves and the axes correspond to rates of $\gamma\tilde{\nu}\bar{\tilde{\nu}}$ production that exceed 1 (curves (a), (c)) or 3 (curves (b), (d)) events for an integrated luminosity of 100 pb^{-1} and fitting with certain kinematic cuts explained in the text.

REFERENCES

|1| E. Fernández et al, Phys. Rev. Lett. 54 (1985) 1118.

|2| J.A. Grifols, X. Mor-Mur and J. Solà, Phys. Lett. 114B (1982) 35.

|3| P. Fayet, Phys. Lett. 117B (1982) 460.

|4| J. Ellis and J.S. Hagelin, Phys. Lett. 122B (1982) 303.

|5| J. Hagelin, G.L. Kane and S. Raby, LA-UR-83-3711 (1983).

|6| L. Ibáñez, FT-UAM-83-28 (1983).

|7| R.Arnowitt, A.H. Chamseddine and P. Nath, Phys. Rev. Lett. 49 (1982) 970; 50 (1983) 232.

|8| J.D. Ware and M.E. Machacek, Phys. Lett. 147B (1984) 415.

|9| M.J. Jonker , talk given at the DESY Workshop (October 1985).

|10| For a detailed discussion see e.g. H.E. Haber and G.L. Kane, Phys. Rep. 117C (1985) 75.

|11| G.P. Lapage, Journal of Computational Phys. 27 (1978) 192.

|12| G. Barbiellini, B. Richter and J.L. Siegrist, Phys. Lett. 106B (1981) 414.

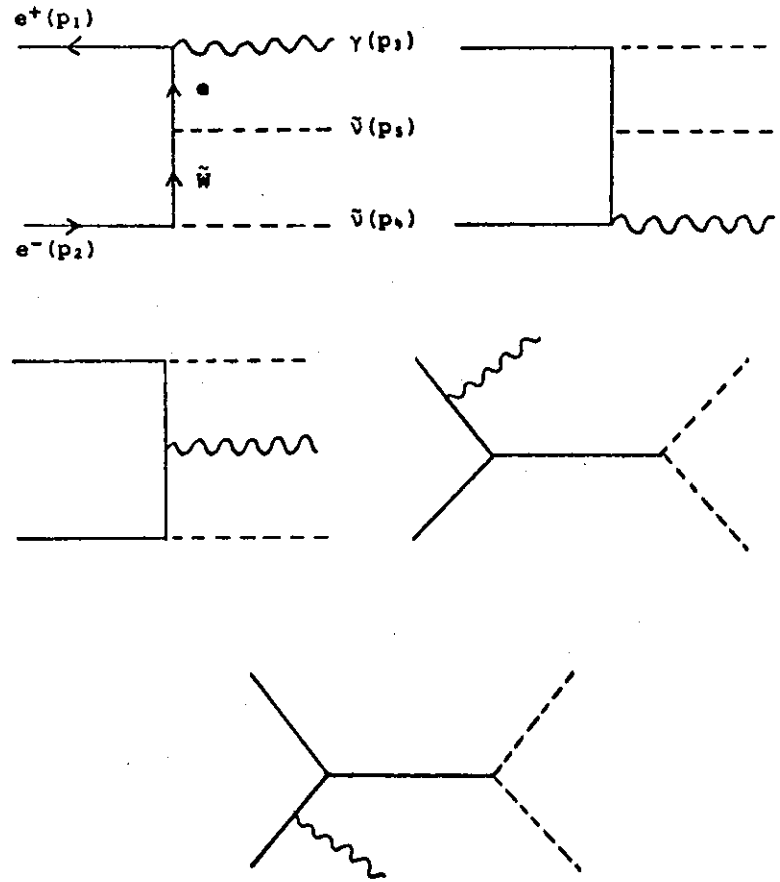

FIG. 1

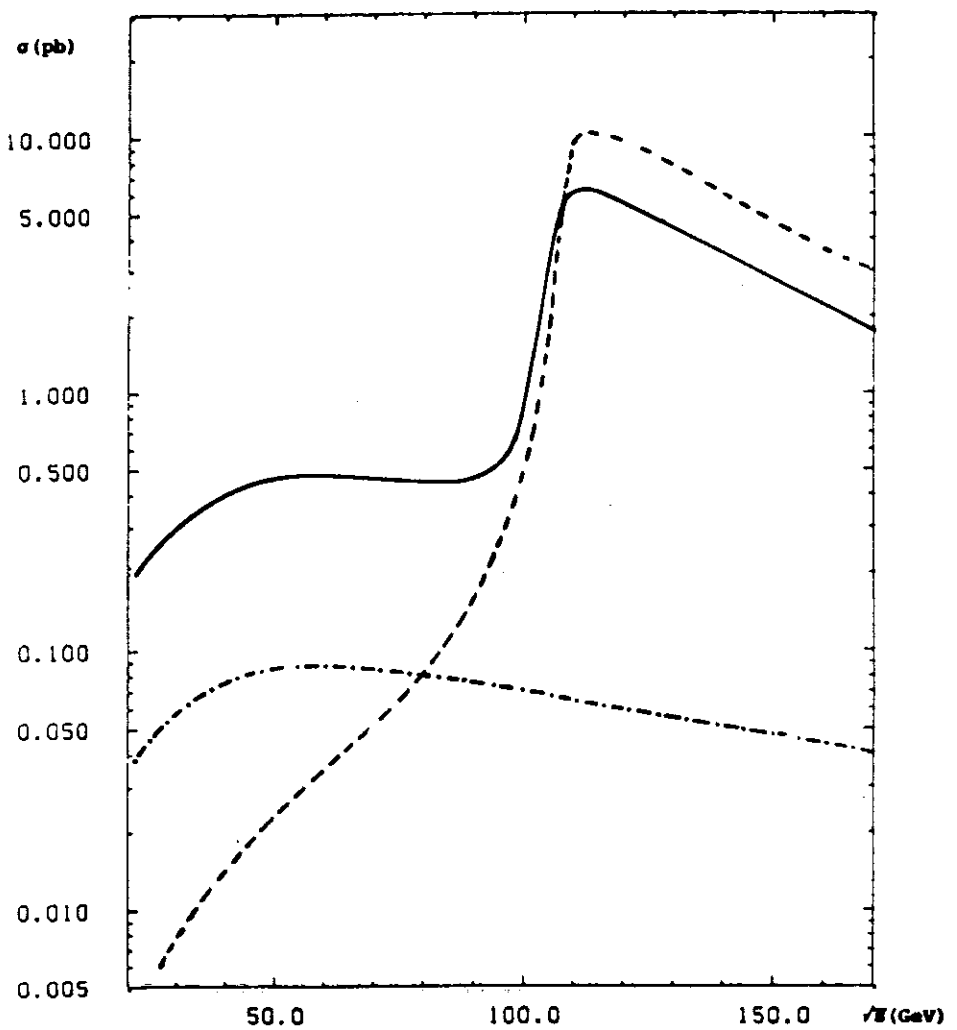

FIG. 2

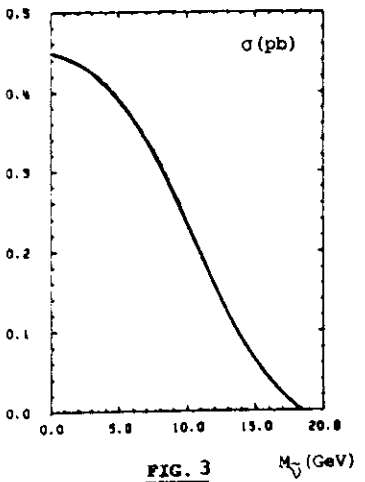

FIG. 3

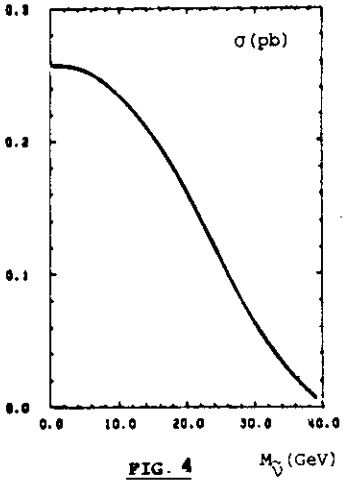

FIG. 4

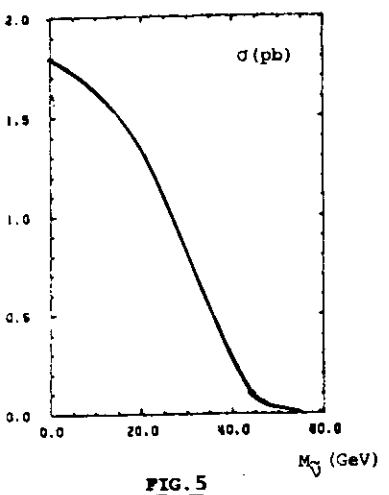

FIG. 5

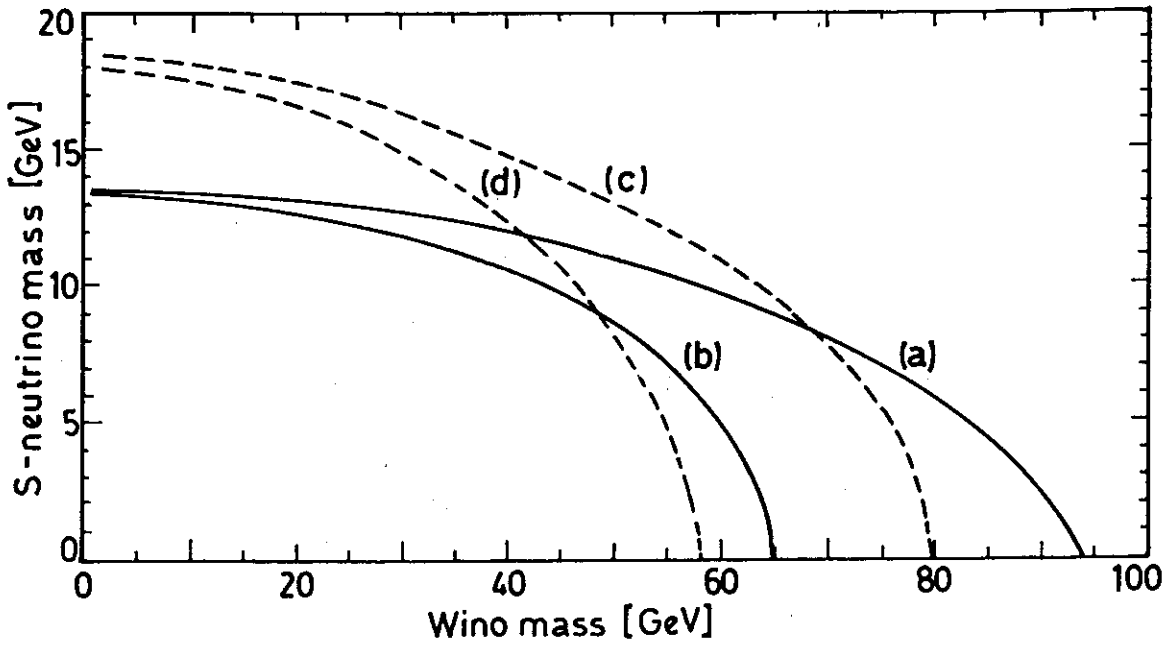

Fig.9

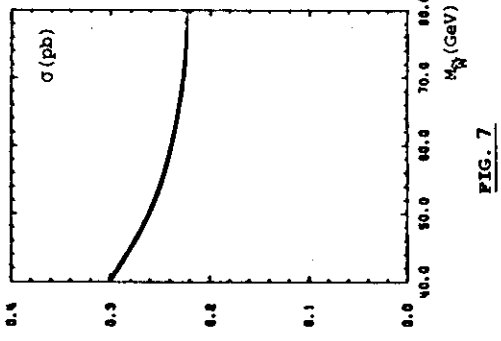

FIG. 7

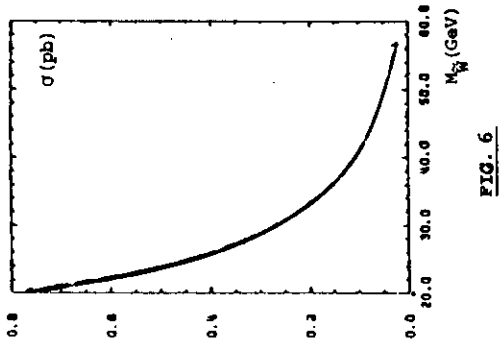

FIG. 6

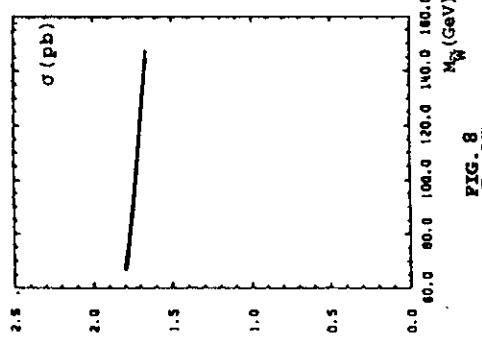

FIG. 8